Available online at www.sciencedirect.com
SCIENCE DIRECT®
Journal of Colloid and Interface Science 275 (2004) 523–529
JOURNAL OF Colloid and Interface Science
www.elsevier.com/locate/jcis

Surface charge properties of Fe_2O_3 in aqueous and alcoholic mixed solvents

S. Mustafa,* S. Tasleem, and A. Naeem

National Centre of Excellence in Physical Chemistry, University of Peshawar, Peshawar, Pakistan

Received 4 November 2003; accepted 26 February 2004

Available online 9 April 2004

Abstract

Iron oxide (Fe_2O_3) was identified and characterized by surface area, X-ray diffractometry, and FTIR analyses. Surface charge densities, point of zero charge (PZC), and surface ionization constants were determined from the potentiometric titration data in various aqueous and aqueous organic mixed solvents in the temperature range 293–313 K. The surface charge densities were observed to decrease with the increase in temperature and concentration of metal ions in both the aqueous and aqueous organic mixed solvents. The absolute values of the surface charge density were found to change in the order aqueous > aqueous/methanol > aqueous/ethanol. Further, the PZC of the iron oxide was observed to shift to the higher pH values in the order ethanol > methanol > aqueous solution, which indicated a decrease in the acidity of the surface –OH groups. The pK_{a_1} and pK_{a_2} values of iron oxide were also determined and then used for determination of the surface potential (ψ_0) of the solid in aqueous and aqueous organic mixed solvents. The surface potential–surface charge curves generally supplemented the results derived from ψ_0–pH curves.

Keywords: Point of zero charge; Surface charge density; Surface potential; Differential capacity; Fe_2O_3

1. Introduction

Metal oxides/hydrous oxides are naturally occurring discrete minerals or in the form of coatings on other particles and exist in various amorphous and crystalline forms [1–5]. In aqueous suspensions they develop surface electrical charges from the dissociation of the surface hydroxyl groups and complexation of the background electrolyte ions. The formation of surface charge is connected with proton balance between the surface of the oxide and the solvent, and its equilibrium is determined by acid–base properties of both the hydroxyl surface groups and the solvent molecules.

Point of zero charge (PZC) is defined as the pH at which the absolute value of the surface charge becomes equal to zero:

$$\sqrt{H^+} - \sqrt{OH^-} = 0. \quad (1)$$

The sign of the surface charge and its magnitude depend on the pH and electrolyte concentration of the ambient solution [4]. Parks and DeBruyan [5] first studied the surface charge of hydrous oxides by using potentiometric titration techniques. According to them, H^+ and OH^- are considered to be the potential-determining ions for hydrous oxides. These studies established the importance of pH and the ionic strength of the electrolyte medium to the sign and magnitude of the surface charge of oxides/hydroxides.

To understand comprehensively the charge development process at the oxide/solution interface, it is necessary to understand the effect of solvent composition on the same. Szezypa et al. [6] observed a decrease in the surface charge–pH curves for rutile/water–ethanol solution in NaCl, but with no shift in the PZC of the solid. Similar results were obtained by Janusz et al. [7] for the TiO_2/water ethanol system. In contrast, Kosmulski et al. [8] found that the PZC for alumina increased from 8.43 to 8.90, and that for rutile from 5.97 to 6.13, when the concentration of dioxane was increased from 0 to 40%.

As such, the behavior of oxides/hydroxides in mixed solvents, i.e., water + organic, is largely unknown and the work reported until now in the literature is rather scanty and inconclusive.

The present work is a comprehensive study of the surface charge properties of α-Fe_2O_3 as a function of temperature

* Corresponding author. Fax: 092-91-9216671.
E-mail address: smustafa49@yahoo.com (S. Mustafa).

0021-9797/$ – see front matter
doi:10.1016/j.jcis.2004.02.089

in the presence of different aqueous and aqueous/alcoholic mixed solvents. Such studies are important as not only are the organic solvents themselves well-known pollutants, but their presence has a profound effect on the interaction of metal cations with the oxides/hydroxides.

2. Experimental

2.1. Reagents

Analytical-grade reagents were used without further purification. Deionized water was used throughout this work. All the solutions were prepared in Pyrex glass vessels. Chlorides of hydrogen, potassium, and iron oxide were supplied by Merck and BDH.

2.2. Characterization of iron oxide

The surface area of the iron oxide was measured by the nitrogen adsorption method [9] using a surface area and pore size analyzer, Model ST-03. An air-dried sample of iron oxide was subjected to X-ray analysis using a JEOL X-ray diffractometer, Model JDX-7E, with Mn-filtered Cu$K\alpha$ radiation. The FTIR spectrum of the sample was taken with a FTIR spectrometer, Perkin Elmer Model 16PC, after mixing a small quantity of Fe_2O_3 with KBr and grinding it into a fine powder.

2.3. Potentiometric titrations of iron oxide

Potentiometric titrations of iron oxide samples in aqueous and aqueous alcoholic media were performed in a thermostated double-walled Pyrex cell of 100-ml capacity with a rubber lid equipped with holes for electrode and microburette and connected to a water bath via a water circulating pump. The temperature of the cell was kept constant at 20, 30, and 40 ± 1 °C.

One-tenth gram of Fe_2O_3 in 40 ml of 10^{-3} M KCl solution as a background electrolyte was placed in the double-walled Pyrex cell and was equilibrated for 30 min with constant stirring by means of a magnetic stirrer. Following equilibration at the desired temperature the initial pH of the solution was adjusted to the desired pH 4 by the addition of either 0.1 M HCl or 0.1 M KOH. The suspension was equilibrated for another 10 min and the pH of the suspension was then measured with an Orion Model 710A pH meter with a combination of pH electrodes of research grade. The standardized solution of 0.01 M KOH was added by means of a microburette with a very fine capillary tip in increments of 0.2 ml. The suspension pH was recorded every 2 min as a function of volume of titrant added until the pH reached 10.

In the case of aqueous organic mixed solvents, all experimental procedures were the same as described above, except that 10% methanol and ethanol were also added to the aqueous solution.

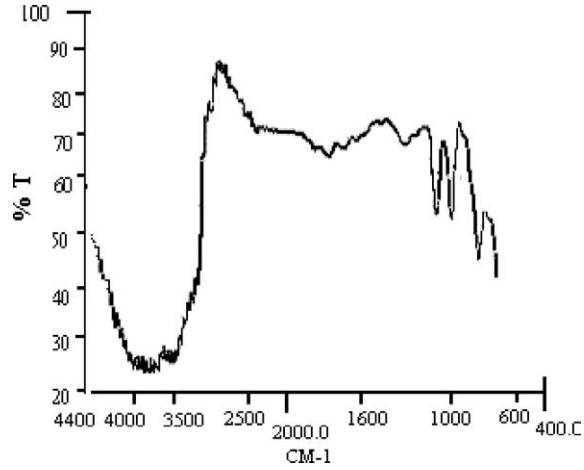

Fig. 1. FTIR spectrum of Fe_2O_3.

3. Results and discussion

3.1. Characterization of iron oxide

The surface area of the Fe_2O_3 was found to be 265 m^2/g. The X-ray diffractogram showed major interplaner spacing at 2.680, 2.560, 2.510, 2.257, 1.714, and 1.685 Å, indicating that the solid sample consisted mainly of synthetic hematite Fe_2O_3. The results obtained here are similar to those reported elsewhere [10].

The FTIR spectrum of dried Fe_2O_3 is given in Fig. 1 and reveals five major bands at 604, 790, 900, 1640, and 3826 cm^{-1}. The band at 3826 cm^{-1} is assigned to OH stretching vibration and the one at 1640 cm^{-1} to the OH bending vibration of surface OH groups. The band at 604 cm^{-1} represents the Fe–O vibration, whereas the bands at 790 and 900 cm^{-1} can be assigned to the Fe–OH vibration as reported elsewhere [9].

3.2. Solvent effect on surface charge density

The surface charge densities of Fe_2O_3 in aqueous and aqueous alcoholic mixed solvents are presented in Figs. 2–5 and were calculated from the potentiometric data using the relationship

$$\delta_0 = \frac{(C_a - C_b + [OH^-] - [H^+])}{m}, \tag{2}$$

where δ_0 = surface charge (μmol/g), C_a and C_b = concentrations (mol/dm^3) of acid and base after addition to the iron oxide suspension, m = mass of iron oxide (g), and $[H^+]$ and $[OH^-]$ are the concentrations of H^+ and OH^- determined from the pH of the solution.

The surface charge data plotted in the form of δ_0–pH curves are presented in Figs. 2–5. It is interesting to observe from the figures that in the pH limit 4–9, there is a linear decrease in surface charge with pH which is then followed by a sharp decrease above pH 9. Further, the surface charge densities decrease with an increase in temperature in both

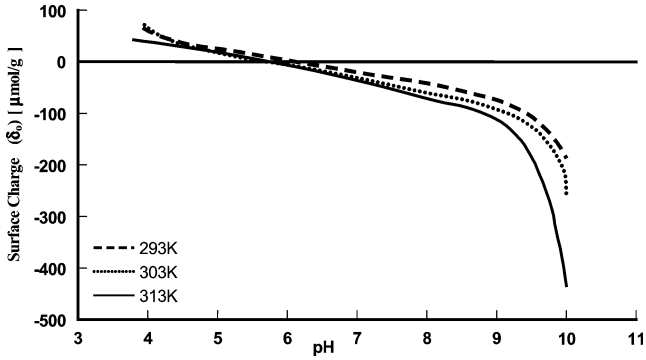

Fig. 2. Variation of the surface charge density of Fe_2O_3 as a function of pH in the presence of K^+ in aqueous solution at different temperatures.

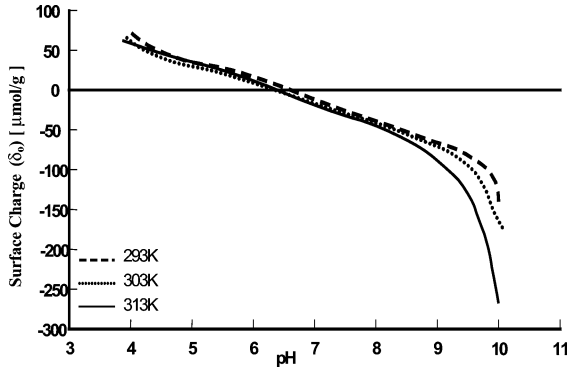

Fig. 3. Variation of the surface charge density of Fe_2O_3 as a function of pH in the presence of K^+ in aqueous methanol solution at different temperatures.

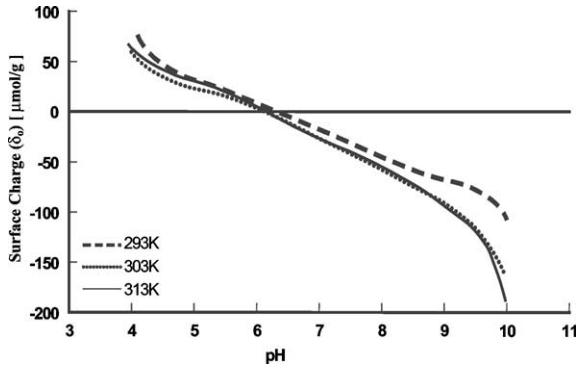

Fig. 4. Variation of the surface charge density of Fe_2O_3 as a function of pH in the presence of K^+ in aqueous ethanol solution at different temperatures.

aqueous and aqueous organic mixed solutions and follow the trend aqueous > aqueous methanol > aqueous ethanol.

The behavior of iron oxide (Fe_2O_3) can be explained if it is assumed that an electrical double layer formed at the oxide/solution interface behaves like a parallel plate condenser with a constant differential capacity according to the well-known theory of Gouy [11] and Chapman [12]. According to this theory

$$\delta_0 = \frac{\varepsilon k}{4\pi}\frac{RT}{F}(\mathrm{PZC} - \mathrm{pH}), \tag{3}$$

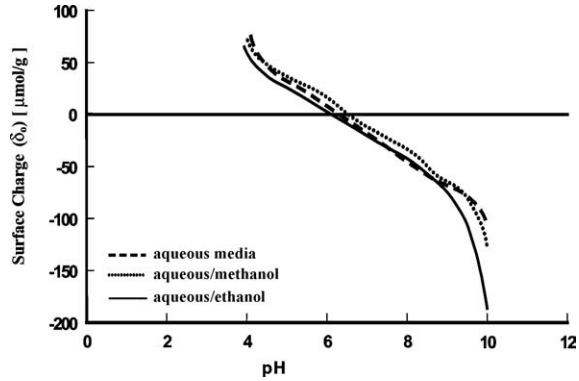

Fig. 5. Variation of surface charge density of Fe_2O_3 as a function pH in the presence of K^+ in aqueous/organic mixed solvents at 293 K.

Table 1
Solvent effect on the PZC and surface dissociation constant of iron oxide at different temperatures

System	Temp. (K)	pK_{a_1}	pK_{a_2}	PZC	
				Exp.	Calc.
Aqueous media	293	5.40	7.16	6.20	6.30
	303	4.54	6.99	5.80	5.80
	313	4.77	7.78	5.70	6.20
Aqueous/methanol	293	5.87	7.84	6.70	6.80
	303	5.50	7.59	6.50	6.50
	313	5.64	7.74	6.50	6.60
Aqueous/ethanol	293	5.89	7.21	6.40	6.50
	303	5.37	7.27	6.20	6.25
	313	6.61	6.94	6.20	6.70

where ε = electronic charge, k = the Debye reciprocal length parameter, ψ_0 = mean potential in the plane of the surface charge (δ_0). For a constant value of k, $\varepsilon k/4\pi$ will be constant and equal to the capacity of a parallel plate condenser. However, this is possible only when the background electrolyte behaves as an inert electrolyte having no specific adsorption at the interface; i.e., counterions are present only in the outer Helmholtz layer.

The curves in Fig. 2 reveal that at pH values above 9.5, the background electrolyte no longer behaves as an inert electrolyte, probably due to specific adsorption of K^+ ions. The δ_0–pH curves also indicate that the structure of the double layer in the aqueous methanol and aqueous ethanolic solution is almost similar to that in the aqueous solution except that in the mixed solvents the specific adsorption of K^+ ion above pH 9 is reduced considerably.

3.3. Effect of temperature on point of zero charge (PZC)

The PZC values determined from the δ_0–pH curves at different temperatures for aqueous and aqueous organic mixed solvents are presented in Table 1, which shows a decrease in the values of PZC with increase in temperature for all the cases under investigation. This decrease in the PZC of iron oxide observed in the present investigation is in agreement with the results of Tewari and Mclean [13], Tewari and

Campbell [14], Janusz et al. [15], and Mustafa et al. [16,17]. The effect of temperature on the PZC of the oxide may be due to changes in the ionization of water, changes in the concentrations of SOH_2^+ and SO^- groups of the solid, and changes in specific adsorption of the ion of the background electrolyte. The KCl used as a background electrolyte in the present investigation is reported in the literature [18,19] to be an inert one; i.e., the specific adsorption of both K^+ and Cl^- is almost negligible. Similarly, the change in $1/2\ pK_w$ in the temperature range 293–313 K is equal to 0.35, which is lower than the observed decrease in the PZC value of iron oxide, equal to 0.5. As such, it is the change in the affinity of H^+/OH^- ions toward the iron oxide surface that determines the effect of temperature on the PZC.

A number of models have been proposed to describe the behavior of insoluble metal oxides/hydroxides in aqueous solutions: Marinsky [20], Schoonen [21], Zhang et al. [22], Parks and Resalbto [23], and Davis et al. [24]. One of the most popular models, the triple-layer model (TLM) of Davis et al. [24], has been used successfully by many authors using both the linear graphical procedure and the computer program SURFEQL [25]. This method is based on two major assumptions.

1. At low electrolyte concentration the surface charge arises from the amphoteric ionization of the surface hydroxyl groups as

$$SOH_2^+ \overset{K_{a_1}\ (\text{int})}{\longleftrightarrow} SOH + H^+, \tag{4}$$

$$SOH \overset{K_{a_2}\ (\text{int})}{\longleftrightarrow} SO^- + H^+. \tag{5}$$

2. At moderately high electrolyte concentrations, the complexation of the electrolyte ions with the surface charge sites dominates over surface ionization and may account for a major fraction of total surface charge.

For an oxide in KCl, as in the present case, the surface charge also arises from the reactions

$$SOH_2^+ + Cl^- \overset{\text{KCl (int)}}{\longleftrightarrow} SOH_2^+ \cdots Cl^-, \tag{6}$$

$$SO^- + K^+ \overset{\text{KCl (int)}}{\longleftrightarrow} SO^- \cdots K^+, \tag{7}$$

where S denotes the surface. Davis et al. [24] derived the following relationships for calculating these constants:

$$pK_{a_1}^{\text{int}} = pH + \log\left(\frac{\alpha^+}{1-\alpha^+}\right) + \frac{e\psi_0}{2.303KT} = pQ_{a_1} + \frac{e\psi_0}{2.303KT}, \tag{8}$$

$$pK_{a_2}^{\text{int}} = pH - \log\left(\frac{\alpha^-}{1-\alpha^-}\right) + \frac{e\psi_0}{2.303KT} = pQ_{a_2} + \frac{e\psi_0}{2.303KT}. \tag{9}$$

Here $\alpha^+ = \delta^+/\delta$ (max), $\alpha^- = \delta^-/\delta$ (max), δ_0 = surface charge density ($\mu C/cm^2$), e = electric charge, K = Boltzman's constant, T = absolute temperature, ψ_0 = mean potential in the plane of the surface charge (δ_0), and the bracketed terms represent the concentrations of the species in the bulk of the solution. Since the value of the surface potential (ψ_0) is not known throughout the pH range with the exception of the PZC, where it is equal to zero, it is difficult to determine the values of pK_{a_1} and pK_{a_2} directly from Eqs. (8) and (9). However, the numerical values of pK_{a_1} and pK_{a_2} may be obtained by plotting $pH + \log(\alpha^+/(1-\alpha^+))$ and $pH - \log(\alpha^-/(1-\alpha^-))$ as a function of α^+ and α^-, respectively, and by extrapolating to $\alpha^{\pm} = 0$. However, in the present case it is clear from Figs. 6–9 that no linear extrapolation is possible. The values of pK_{a_1} and pK_{a_2} determined from the extrapolation using the computer program Excel 0.5 of the function pQ_{a_1} and pQ_{a_2} are presented in Table 1. Table 1 also lists the PZC values estimated from the well-known relationship [26,27]

$$\text{PZC} = \frac{pK_{a_1} + pK_{a_2}}{2}. \tag{10}$$

It is quite clear from the table that there is good agreement between the values of PZC determined from the potentiometric titration and those calculated from Eq. (10). The

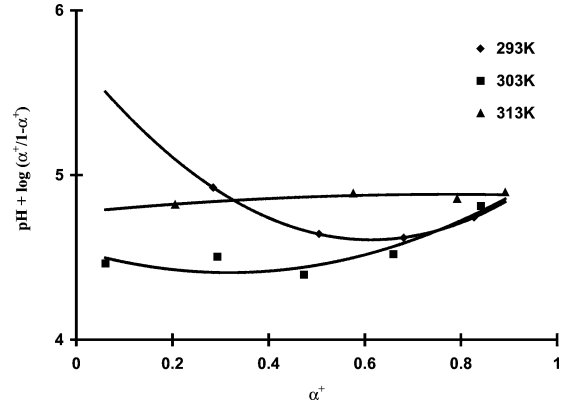

Fig. 6. Plots of $pH + \log(\alpha^+/(1-\alpha^+))$ as a function of fractional surface ionization (α^+) for Fe_2O_3 in the presence of K^+ in aqueous solution at different temperatures.

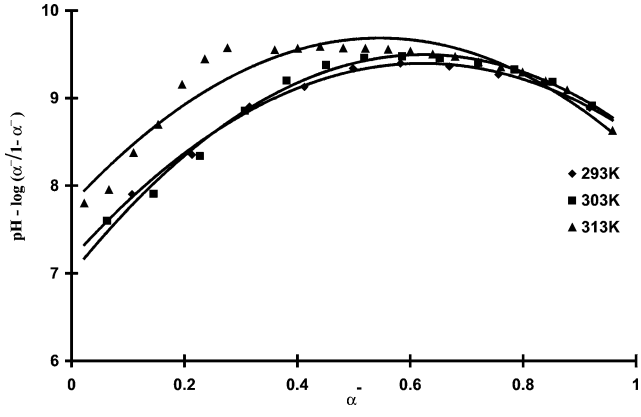

Fig. 7. Plots of $pH - \log(\alpha^-/(1-\alpha^-))$ as a function of fractional surface ionization (α^-) for Fe_2O_3 in the presence of K^+ in aqueous solution at different temperatures.

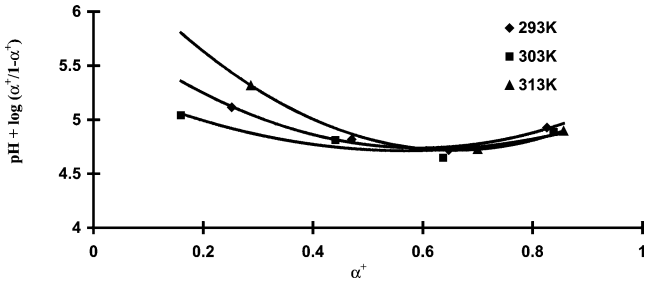

Fig. 8. Plots of $\mathrm{pH} + \log(\alpha^+/(1-\alpha^+))$ as a function of fractional surface ionization (α^+) for Fe_2O_3 in the presence of K^+ in aqueous/ethanol solution at different temperatures.

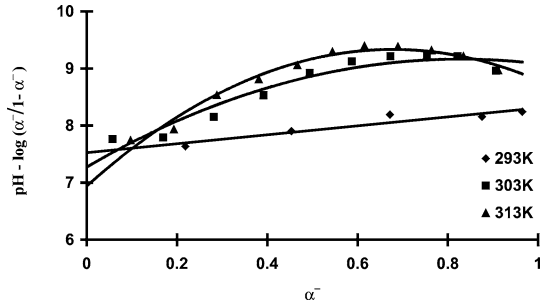

Fig. 9. Plots of $\mathrm{pH} - \log(\alpha^-/(1-\alpha^-))$ as a function of fractional surface ionization (α^-) for Fe_2O_3 in the presence of K^+ in aqueous/ethanol at different temperatures.

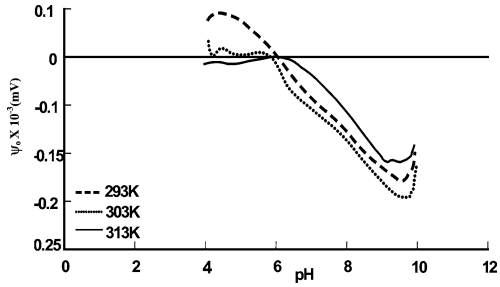

Fig. 10. Plots of ψ_0 as a function of pH for Fe_2O_3 in the presence of K^+ in aqueous solution at different temperatures.

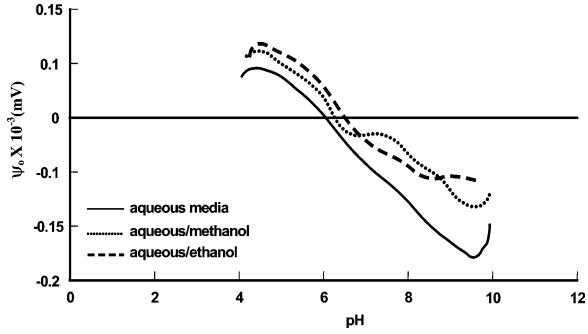

Fig. 11. Plots of ψ_0 as a function of pH for Fe_2O_3 in the presence of K^+ in aqueous/organic mixed solvents at 293 K.

values of both pK_{a_1} and pK_{a_2} decrease with the increase in temperature from 293 to 303 K (Table 1), which suggests that the deprotonation process of SOH_2^+, SOH illustrated in reactions (4) and (5) increases with the increase in temperature. The effect of the presence of alcohols in the system can also be seen from the increase in pK values in the order aqueous $<$ 10% methanol $<$ 10% ethanol solution, showing that the deprotonation process decreases when methanol and ethanol are added to the system. A similar trend in the variation of the surface acidity constants pK_{a_1} and pK_{a_2} with temperature was observed by Blesa et al. [28] for magnetite surface in aqueous electrolyte solutions.

3.4. Solvents and temperature effect on ψ_0–pH curves

The pK_{a_1} and pK_{a_2} values given in Table 1 were used to determine the values of the surface potential (ψ_0) according to the method given by Sprycha and Szezypa [29]. The results are presented in Figs. 10 and 11. Fig. 10 shows a linear decrease in electrical potential (ψ_0) with pH between the pH limits 5.8 and 9.5. This is possible only as discussed earlier if the background electrolyte behaves as an inert electrolyte having no specific adsorption at the interface. However, at pH values above 9.5 and below 5.8, the background electrolyte ceases to behave as an inert electrolyte due to strong specific adsorption of K^+ and Cl^- ions. It can also be seen from the ψ_0–pH curves that the K^+ ion has a much stronger effect than the Cl^- ion in the charging mechanism of the iron oxide. Further, with the increase in temperature, the role of both the K^+ and Cl^- ions increases due to their increased adsorption as the ions move into the inner Helmholtz layer. This interpretation of the double layer is in agreement with the three-layer model of the oxide/solution interface developed by Machesky et al. [30]. The ψ_0–pH curves for mixed solvents in Fig. 11 also indicate that the structure of the double layer in the aqueous methanol and aqueous ethanolic solutions is almost similar to that in the aqueous solution, except that in the mixed solvents the specific adsorption of anions is considerably reduced.

3.5. Effect of organic solvents and temperature on ψ_0–δ_0 curves

The ψ_0–δ_0 curves given in Figs. 12 and 13 generally supplement the results derived from ψ_0–pH curves. The slopes of these curves give information regarding the differential capacities of the electrical double layer. The straight-line behavior of the curves in the PZC region show that the differential capacities of the electrical double layer are almost constant and increase or decrease only when sorption of cation or anion takes place. The values of differential capacities in the PZC region are given in Tables 2 and 3. As can be seen there is a slight increase in the values of differential capacity with increase in temperature. Such an increase in the differential capacity is probably due to the decrease in Debye length (k) as more of the ions of the background electrolyte move into the inner Helmholtz layer [31]. However, the increase in differential capacity in mixed aqueous/organic solvent is not easily understandable, as the sorption of the organic molecule into the double layer is expected to decrease

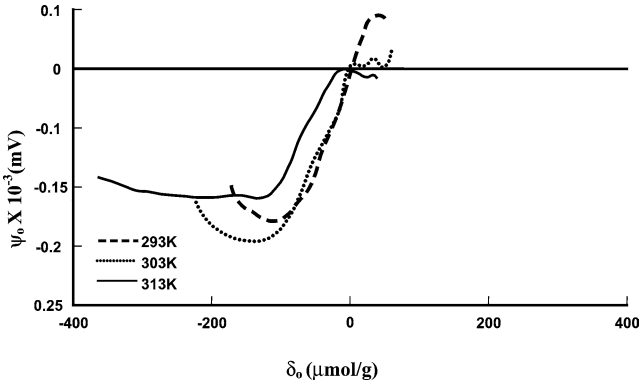

Fig. 12. Plots of ψ_0 as a function surface charge density in the presence of K^+ in aqueous solution at different temperatures.

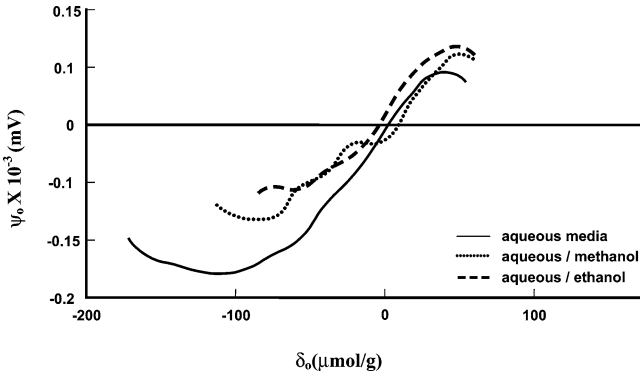

Fig. 13. Plots of ψ_0 as a function of surface charge density in the presence of K^+ in aqueous and aqueous organic mixed solvents at 293 K.

its values due to a decrease in the dielectric constant of the interfacial region. However, it seems from the present investigation that the dielectric constant plays an insignificant role in the charging mechanism of the oxides/hydroxides. Such a minor role is understandable, if there is only a very slight variation in the dielectric constant of the interfacial region when an aqueous solution is replaced by mixed aqueous organic solution. Devanthan [32] and Devanthan and Tilak [33] derived a value of 7.2 for the dielectric constant of the interfacial water. With such a low value, the addition of 10% methanol or ethanol is expected to have a very little effect on the interfacial dielectric constant probably due to the close packing of the interfacial water.

3.6. Thermodynamics parameters of surface dissociation

The values of ΔG^0 calculated from the well-known thermodynamic relationship $\Delta G^0 = -RT \ln K$ are given in Table 4. The ΔG^0 values are found to be positive at different temperatures in both aqueous and mixed solvents and are found to be in the range 27–45 kJ/mol. The positive values of ΔG^0 show the nonspontaneity of the process which is probably due to the fact that the H^+ ions are highly hydrated in both aqueous and aqueous organic mixed solvents [34]. Similar positive values of ΔG^0 were also found for the dissociation process elsewhere [14].

Table 2
Variation in differential capacity (C) of iron oxide with temperature in aqueous media

No.	Temp. (K)	Differential capacity, C ($\mu F\,cm^{-2}$)
1	293	27
2	303	30
3	313	35

Table 3
Variation in differential capacity (C) of iron oxide with organic solvents at 293 K

No.	System	Differential capacity, C ($\mu F\,cm^{-2}$)
1	Aqueous media	27
2	Aqueous/methanol	33
3	Aqueous/ethanol	40

Table 4
Free energy changes of K^+ exchanged on iron oxide

System	Temp. (K)	ΔG^0 ($kJ\,mol^{-1}$)	
		Positive side	Negative side
Aqueous media	293	29.35	39.21
	303	28.44	42.38
	313	27.52	45.55
Aqueous/methanol	293	32.47	43.38
	303	32.87	44.55
	313	33.28	45.72
Aqueous/ethanol	293	31.36	40.68
	303	34.54	41.27
	313	37.72	41.86

4. Conclusions

From the foregoing discussion, it can be concluded that the addition of alcohols to the aqueous solution has a profound effect on the surface charge properties of Fe_2O_3. The magnitude of surface charge density follows the order aqueous > aqueous/methanol > aqueous/ethanol, while the PZC values vary as ethanol > methanol > aqueous solution, showing a decrease in the acidity of the surface OH groups of the oxide. The electrical double layer formed at the oxide/solution interface behaves like a parallel plate condenser with constant differential capacity in both aqueous and aqueous organic mixed solvents. The differential capacities were found to increase with the increase in temperature as result of movement of the ions of the background electrolyte from the outer Helmholtz to the inner Helmholtz of the electrical double layer.

References

[1] C.H. Lia, C.Y. Chen, B.L. Wei, S.H. Yeh, Water Res. 36 (2003) 4943.
[2] M. Abdulkarim, N. Darwish, Y. Magdy, A. Dwaidar, Eng. Life Sci. 2 (2002) 161.
[3] K. Lackovic, M.L. Angove, J.D. Wells, B.B. Johnson, J. Colloid Interface Sci. 257 (2003) 31.

[4] S. Mustafa, P. Shahida, A. Naeem, B. Dilara, Langmuir 18 (2002) 2254.
[5] G.A. Parks, P.L. DeBruyn, J. Phys. Chem. 66 (1962) 967.
[6] J. Szezypa, A. Sworska, M. Kosmulski, J. Colloid Interface Sci. 126 (1988) 552.
[7] W. Janusz, A. Sworska, J. Szezypa, J. Colloid Interface Sci. 152 (1999) 223.
[8] M. Kosmulski, J. Matyisiak, J. Szezypa, Bull. Pol. Acad. Sci. Chem. 41 (1993) 4.
[9] S. Mustafa, B. Dilara, K. Nargis, A. Naeem, P. Shahida, Colloids Surf. A 205 (2002) 273.
[10] P. Bayliss, L.G. Berry, D.K. Smith, Mineral Powder Diffraction, in: File Data Book, JCPDS, International Centre for Diffraction Data, Pennsylvania, 1980, pp. 364, 789.
[11] L. Gouy, J. Phys. 4 (1910) 457.
[12] P.L. Chapman, Philos. Mag. 6 (1913) 475.
[13] P.H. Tewari, A.W. Mclean, J. Colloid Interface Sci. 40 (1972) 267.
[14] P.H. Tewari, A.B. Campbell, J. Colloid Interface Sci. 55 (1976) 531.
[15] W. Janusz, A. Sworska, J. Szezypa, Colloids Surf. A 149 (1999) 421.
[16] S. Mustafa, B. Dilara, A. Naeem, J. Colloid Interface Sci. 204 (1998) 284.
[17] S. Mustafa, A. Hamid, A. Naeem, S. Murtaza, Phys. Chem. 14 (2003) 1.
[18] C. Katerina, L.V. Akratopulu, A. Lycourghiotis, J. Chem. Soc. Faraday Trans. 82 (1986) 3697.
[19] M.A. Anderson, A.J. Rubin, Adsorption of Inorganic at Solid Liquid Interface, Ann Arbor Science, Ann Arbor, MI, 1981, ch. 1.
[20] J.A. Marinsky, J. Phys. Chem. 100 (1996) 1858.
[21] M.A.A. Schoonen, Geochim. Cosmochim. Acta 58 (1994) 2845.
[22] Q. Zhang, Z. Xu, J.A. Finch, J. Colloid Interface Sci. 169 (1995) 414.
[23] I. Parks, R. Resalbto, J. Colloid Interface Sci. 175 (1995) 239.
[24] J.A. Davis, R.O. James, J.O. Leckie, J. Colloid Interface Sci. 63 (1978) 480.
[25] N. Spanos, S. Slaror, C. Kordulis, A. Lycoughiotis, Langmuir 10 (1994) 3134.
[26] W. Stumm, J.J. Morgan, Aquatic Chemistry, second ed., Wiley, New York, 1981, p. 631.
[27] L. Vordonis, P.G. Koutsoukos, A. Lycourghiotis, J. Catal. 98 (1986) 296.
[28] M.A. Blesa, N.M. Figliolia, A.J.G. Maroto, A.E. Regazzoni, J. Colloid Interface Sci. 101 (1984) 410.
[29] R. Sprycha, J. Szezypa, J. Colloid Interface Sci. 102 (1984) 288.
[30] M.L. Machesky, D.J. Wesolowski, D.A. Palmer, K.I. Hayahi, J. Colloid Interface Sci. 200 (1998) 298.
[31] A. Kitahara, A. Watanabe, Electrical Phenomena at Interface, Dekker, New York/Basel, 1984.
[32] M.A.V. Devanathan, Trans. Faraday Soc. 50 (1954) 373.
[33] M.A.V. Devanathan, B.V.K.S.R.A. Tilak, Chem. Rev. 65 (1965) 635.
[34] S. Mustafa, A. Naeem, N. Rehana, T. Hussain, J. Colloid Interface Sci. 220 (1999) 63.